Mutations in Paired α-Helices at the Subunit Interface of Glycogen Phosphorylase Alter Homotropic and Heterotropic Cooperativity†

Jenny L. Buchbinder,‡ Joan J. Guinovart,§ and Robert J. Fletterick*,‡

Department of Biochemistry and Biophysics, University of California, San Francisco, San Francisco, California 94143-0448

Received October 24, 1994; Revised Manuscript Received February 16, 1995⊗

ABSTRACT: Allosteric switching between inactive and active conformational states in muscle glycogen phosphorylase alters the pattern of van der Waals contacts and hydrogen bonds between two helices located at the dimer interface of the enzyme. Alanine was substituted for residues N270, N274, and R277 to perturb helix interactions, which differ in inactive and active conformations. In addition, the entire α-helix in each subunit was exchanged with the analogous region from yeast phosphorylase. The N274A mutant shows increased affinity and reduced cooperativity for the activator, AMP, and reduced cooperativity for the substrate, glucose 1-phosphate. The N270A and R277A mutants, in contrast, show reduced binding and cooperativity for AMP and relatively little change in binding or cooperativity for glucose 1-phosphate. The substitution of the helix from the yeast enzyme results in an 8-fold reduction in V_{max}, a loss in cooperativity for both AMP and glucose 1-phosphate, but little change in the affinities of either ligand. Crystallographic analyses of the N274A and R277A mutants show that these substitutions cause only small changes in the structure of the unliganded, inactive form of phosphorylase. The substitution at N274 eliminates intersubunit interactions which selectively stabilize the enzyme in an inactive conformation. The kinetic results indicate that the mutations at N270 and R277, on the contrary, perturb packing interactions at the dimer interface of the activated enzyme and weaken binding of AMP. The relatively modest effects of the replacement with the helices from the yeast enzyme indicate that the helices are not crucial for catalytic function.

Interest in the mechanism of allosteric regulation of glycogen phosphorylase began with the discovery decades ago of the requirement by the enzyme of AMP for activation (Cori & Cori, 1936). The question remains of precisely how effector binding energy in this allosteric enzyme is coupled to structural rearrangements throughout the protein to bring about changes in ligand affinities and levels of catalytic activity. Glycogen phosphorylase catalyzes the first step in the glycogen degradation pathway, the phosphorolysis of α-1,4-glycosyl linkages of glycogen to give glucose 1-phosphate. The enzyme isolated from skeletal muscle responds to a variety of allosteric effectors besides the activator AMP, including the inhibitors ATP, ADP, glucose 6-phosphate, glucose, and purine-like compounds (Morgan & Parmeggiani, 1964; Parmeggiani & Morgan, 1962; Cori & Cori, 1940; Kihlman & Overgaard-Hansen, 1955). In addition, the enzyme is activated by phosphorylation at a serine residue near its N-terminus (Fischer & Krebs, 1955; Krebs & Fischer, 1956; Fischer et al., 1959). The phosphorylation state of the enzyme is determined by the competing actions of phosphorylase kinase and protein phosphatase PP1 whose activity levels are controlled by extracellular neuronal and hormonal signals by means of a cyclic-AMP second messenger system (Cori & Green, 1943; Fischer et al., 1957; Krebs, 1972; Ingebritsen & Cohen, 1983; Cohen, 1989).

The enzyme functions as a dimer of identical subunits, each having a molecular mass of 97.4 kDa (Huang & Graves, 1970; Buc et al., 1971; Titani et al., 1977). Each subunit can be divided into two domains, which both possess α/β structure: an N-terminal domain comprises amino acid residues 1−482, and a C-terminal domain comprises residues 483−842 (Fletterick & Madsen, 1980; Fletterick & Sprang, 1982; Johnson, 1989). The N-terminal domain contains three of the allosteric sites, a phosphorylation site at Ser 14, an AMP activation site, and a glycogen activation site. Residues from both the C-terminal and the N-terminal domains form the two remaining allosteric sites, a glucose inhibitory site and a purine inhibitory site. The active site lies in a cleft at the interface of the two domains.

Structural changes associated with phosphorylation and ligand binding have been identified from crystallographic studies of phosphorylated and unphosphorylated forms of phosphorylase in complexes with substrates and effectors (Johnson, 1992; Browner & Fletterick, 1992; Johnson & Barford, 1990; Fletterick & Madsen, 1980; Fletterick et al., 1986; Johnson, 1989). Crystallographic structures show that the enzyme adopts multiple conformational states, which range from the inactive conformer of the unphosphorylated enzyme complexed with inhibitors to that of the fully activated phosphorylated enzyme saturated with AMP. In between these structural extremes lie partially activated conformers in which a portion of the N-terminal subdomain assumes an activated conformation but the active site remains inhibited (Sprang et al., 1988). Conformational differences among the crystallographic structures have been analyzed

† This work was supported by NIH Grant DK32822 to R.J.F., NIH postdoctoral fellowship GM15371 to J.L.B., and a sabbatical fellowship from CICYT to J.J.G.

* To whom correspondence should be addressed.

‡ University of California.

§ Permanent address: Department de Bioquimica, Facultad de Quimica, University of Barcelona, Marti I Franques, 1 E-08028 Barcelona, Spain.

⊗ Abstract published in *Advance ACS Abstracts,* May 1, 1995.

0006-2960/95/0434-6423$09.00/0

quantitatively by using the superpositioning algorithm and more recently by using the less conventional principal axes algorithm in order to define the extents of domain and subunit movements (Browner et al., 1992). The rearrangements in elements of secondary structure that accompany activation have now been described for several conformers in various crystallographic states.

Activation of the enzyme is associated with a large quaternary change in which the two subunits rotate 5° about two axes approximately perpendicular to the molecular two-fold (Sprang et al., 1991; Barford et al., 1991; Goldsmith et al., 1989; Barford & Johnson, 1989; Sprang et al., 1992; Zhou et al., unpublished). Binding of AMP or phosphorylation at serine 14 brings the subunits closer together on the N-terminal side of the dimer interface as salt-bridge and hydrogen bonding interactions form between the allosteric effectors and residues from either subunit (Sprang et al., 1987, 1988; Sprang et al., 1991, 1991). These local rearrangements serve as the trigger for the global changes that constitute the allosteric transition. One of the largest changes in tertiary structure, during the transition, occurs on the catalytic side of the dimer interface where helix α_7 (residues 264−277), referred to as the tower helix, forms contacts with it counterpart in the opposite subunit (Goldsmith et al., 1989; Barford & Johnson, 1989). As a result of the subunit rotation, the tower helices, initially in an approximately antiparallel configuration in the inactive state, move past each other such that the angle formed by the helices crossing each other is about 80°. This change in configuration alters the pattern of intrasubunit and intersubunit contacts among residues of the helices. A loop of amino acids (residues 280−288), which directly follows each tower helix and is referred to as the active site gate, also undergoes a large change in position (Withers et al., 1982; Goldsmith et al., 1989; Barford & Johnson, 1989; Martin et al., 1990). When the enzyme is in an inactive conformation, the active site gate forms interactions with residues of the N-terminal and the C-terminal domains at their interface near the active site and hinders binding of substrates. Upon activation of the enzyme, the N and C domains rotate apart by 5°, and the gate becomes disordered as it moves away from the active site such that it no longer obstructs binding of substrates. Together, conformational changes in the tower helices and the active site gate may be essential for coupling the quaternary structural changes associated with activation by AMP or phosphorylation to tertiary changes which link the two catalytic sites of the dimer.

In the present study, the importance of intrasubunit and intersubunit interactions among residues of the tower helices was evaluated by using site-directed mutagenesis to eliminate hydrogen-bonding interactions formed by side chains of residues N270, N274, and R277. To further test the role of the helices in the allosteric transition, the tower helix region of the muscle enzyme was replaced with the corresponding region of the yeast enzyme. Only 33% of the amino acids are identical in the yeast helix, and residues 270, 274, and 277 are not conserved (Hwang & Fletterick, 1986). Unlike the muscle enzyme, yeast phosphorylase is not activated by AMP (Fosset et al., 1971). The mutants have been analyzed kinetically, to assess the effects of amino acid replacements on activation and ligand cooperativity, and crystallographically, to determine the extents of structural perturbations.

MATERIALS AND METHODS

Materials

Oyster glycogen type II was purchased from Sigma. *Escherichia coli* strain 25A6 was supplied by Genentech Inc. (South San Francisco, CA).

Methods

Mutagenesis. The cDNA of rabbit muscle phosphorylase, cloned into the *E. coli* plasmid pHSe5 (Browner et al., 1991), was used for mutagenesis and enzyme expression. Oligonucleotides required for site-directed mutagenesis, PCR,[1] and DNA sequencing primers were synthesized with an Applied Biosystems PCRmate synthesizer. Alanine substitutions were made at N270, N274, and R277 by oligonucleotide-directed mutagenesis using the procedure of Kunkel with some modifications as described by Browner et al. (1991). Oligonucleotides were 20−38 bases in length and contained base substitutions for introduction of alanine at the appropriate positions and additional base substitutions for introduction of restriction sites neighboring the mutation sites to allow screening DNA for mutations by restriction digests. Conservative base substitutions which did not alter the amino acid sequence were used for introduction of the restriction sites. A DNA fragment coding for the yeast tower helix region (residues 261−281) was generated by PCR. Primers for the PCR reaction were designed to introduce an *Afl*II restriction site on the 5′ end and a *Bst*BI restriction site on the 3′ end of the PCR fragment coding for the yeast tower helix. Corresponding *Afl*II and *Bst*BI sites were introduced into the muscle phosphorylase cDNA by Kunkel mutagenesis. After digestion of the PCR fragment and the muscle phosphorylase cDNA with *Afl*II and *Bst*BI, the PCR fragment was cloned into the muscle phosphorylase cDNA to replace the sequence coding for the muscle tower helix region. For all the enzyme variants, the presence of the desired mutations was verified by dideoxy sequencing of the mutated phosphorylase cDNAs around the mutation sites and in the regions within 300 base pairs flanking the mutations.

Protein Expression and Purification. The mutant constructs were expressed in cultures of *E. coli* strain 25A6 [W3110; *ton*A, *lon*Δ, *qal*E, *htp*P^{ts}] grown at 22 °C under conditions used in the past to express the wild-type enzyme (Browner et al., 1991). Typically, 1 L cultures of *E. coli* yielded 5−15 mg of the enzyme variants. Cell were lysed by sonication, and the mutants were purified by chromatography on Fast-Flow Metal Chelating Sepharose and Fast-Flow DEAE-Sepharose as described previously (Luong et al., 1992). Purified enzyme was stored in 25 mM β-glycerophosphate, 1 mM EDTA, 1 mM DTT, and 50% glycerol at −20 °C. Prior to kinetic analyses or crystallization, enzyme was desalted by chromatography on Sephadex G25.

Assays and Analysis of Kinetic Data. Enzyme concentrations were determined by absorbance measurements at 280 nm using the extinction coefficient for the wild-type enzyme

[1] Abbreviations: EDTA, ethylenediaminetetraacetic acid; DTT, dithiothreitol; IPTG, isopropyl β-D-thiogalactopyranoside; rms, root mean square; $[S]_{0.5(G\text{-}1\text{-}P)}$, glucose 1-phosphate concentration at half the maximal observed specific activity; $[S]_{0.5(AMP)}$, AMP concentration at half the maximal observed specific activity; PCR, polymerase chain reaction; YTH, mutant that has residues 261−281 replaced with those from the tower helix region of yeast phosphorylase.

of 1.32 cm^2/mg (Buc et al., 1971). Glycogen, used in kinetic assays, was purified to remove contaminating phosphate. The glycogen was dissolved in water and passed through a Dowex AG 1-X8 anion exchange column (2.5 × 10 cm). Fractions were pooled and ethanol was added to a final concentration of 66% (v/v) to precipitate the glycogen. The supernatant was then decanted, and the glycogen was dried by lyophilization. The activity of the phosphorylase variants was measured at 30 °C by using a fixed time assay that quantitated the amount of phosphate produced from the reaction of glucose 1-phosphate and glycogen (Carney et al., 1978). The reaction mixtures contained 50 mM BES, pH 6.8, 1 mM EDTA, 1 mM DTT, and 1% glycogen in a final volume of 0.5 mL. AMP was varied in the range of 0−300 μM while the concentration of glucose 1-phosphate was held constant for the determination of the K_a and the Hill coefficient, n_H, of AMP. Similarly, glucose 1-phosphate was varied in the range of 0−10 mM while the concentration of AMP was held constant for the determination of the substrate concentration at half-maximal velocity, $[S]_{0.5}$, and n_H of glucose 1-phosphate. Enzyme was preincubated with assay mixtures containing everything but glucose 1-phosphate for 5 min prior to initiation of the reactions with the substrate. Reaction rates were determined from the measured absorbances at 316 nm. The kinetic data were fit to the Hill equation by nonlinear regression with the program JMP (SAS Institute Inc., 1989). All measurements were performed in quadruplicate, and kinetic parameters are reported along with the standard errors that were calculated by the curve-fitting program.

Crystallization. The N274A and the R277A mutants were crystallized by the vapor diffusion method in hanging drops under conditions similar to those used previously to crystallize the *b* form of the wild-type enzyme (Eagles et al., 1972). Both mutant enzymes crystallized at concentrations of 10−30 mg/mL from solutions of 10 mM BES, 0.1 mM EDTA, and 1.0 mM DTT at pH 7.0 in 10 μL drops equilibrated at 18 °C. Microseeding with crushed crystals of the wild-type enzyme was used to induce the mutants to crystallize more readily and in the same space group as the native enzyme. Initial crystals were too small for diffraction analysis but could be enlarged by macroseeding to dimensions of 0.2 mm × 0.2 mm × 1.5 mm. Diffraction quality crystals of the N270A mutant and the mutant containing the yeast tower helix region could not be obtained and attempts to crystallize the R277A and N274A enzymes in activated conformations were unsuccessful.

X-ray Diffraction Measurements, Data Reduction, and Structure Refinement. The crystals were mounted in glass capillaries for diffraction measurements. Diffraction data for crystals of the N274A mutant were measured using a Siemens multiwire area detector equipped with a three-circle goniostat. Cu Kα radiation was generated with a 12 kW rotating anode operating at 50 kV and 60 mA. Data were reduced with the XDS software package (Kabsch, 1988; Nicolet Instrument Co.). Diffraction data for crystals of the R277A mutant were measured with an Raxis II image plate detector mounted on an 18 kW rotating anode operating at 50 kV and 180 mA. Data for crystals of this mutant were processed with the Raxis II data reduction software package. Crystals of both the N274A and R277A mutants were isomorphous with crystals of native phosphorylase *b*. The structures of both mutants were therefore determined by refining the atomic coordinates from the structure of phosphorylase *b* in the absence of ligands. Structures were refined using the program X-PLOR (Brunger, 1987). Rigid body refinement was performed on the phosphorylase monomer followed by positional refinement, simulated annealing and *B* factor refinement. Electron density maps, calculated with X-PLOR, were displayed on a Silicon Graphics system with the computer graphics program Chain (Sack, 1988), and the positions of individual atoms were adjusted and solvent molecules were added to fit the electron density. In order to properly position mutated residues in the structure, $2F_o - F_c$ omit maps were calculated in which coordinates for the mutated residues and residues neighboring them were absent. Model rebuilding was followed by cycles of positional and *B* factor refinement. In order to establish that the configuration of the tower helices was correct in each mutant structure, annealed omit maps were computed in which an 8.0 Å sphere, centered at the mutated residue, was omitted. Atoms in a 3 Å shell surrounding the sphere were restrained during simulated annealing to prevent their movement into the omitted region. The simulated annealing procedure was initiated at a temperature of 1000 K, and cooling occurred in increments of 25 K until a temperature of 300 K was reached. Annealing was followed by 200 cycles of positional refinement, and omit maps were calculated such that the phases of atoms within the 8.0 Å sphere surrounding the mutated residue were omitted. Finally, individual *B* factors for the entire protein were refined by alternating cycles of positional refinement and *B* factor refinement. Crystal parameters and statistical information about the crystallographic data and the structural refinement of these mutants are shown in Table 1. Electron density in the vicinity of the mutations is shown in Figures 1 and 2.

Table 1: Crystallographic Data and Refinement Statistics

mutant	N274A	R277A
R_{merge} (intensities) all data[a]	8.4%	9.9%
number of reflections	65 002	164 397
number of unique reflections	24 936	46 216
% completeness	73% to 2.5 Å	84% to 2.5 Å (58% for 2.25−2.50 Å) (50% for 2.0−2.25 Å)
space group	$P4_32_12$	$P4_32_12$
cell dimensions	$a = b = 128.3$ Å, $c = 116.1$ Å	$a = b = 128.6$ Å, $c = 116.4$ Å
R_{cryst}[b] (10−2.5 Å)	0.150	0.177
rms deviation from ideal bond lengths	0.014 Å	0.015 Å
rms deviation from ideal bond angles	3.02°	3.19°

[a] $R_{merge} = \sum_i\sum_h|I(h) - I_i(h)|/\sum_i\sum_h I(h)$, where $I_i(h)$, and $I(h)$ are the *i*th and the mean measurement of the intensity of reflection *h*. [b] $R_{cryst} = \sum_h|F_o - F_c|/\sum_h|F_o|$ where F_o and F_c are the observed and caluclated structure factor amplitudes.

Structural Analysis of the Mutants. Structures of the mutants were compared to structures of the wild-type enzyme by superpositioning. First, the program Newdome was used to determine which C_α positions showed the least change in the structures being compared (Perry et al., 1990). Then, the coordinates of "fixed" regions were superimposed, and the rotational and translational displacements of atomic coordinates for backbone atoms were calculated with the program GEM (Fauman, unpublished results). Superimposed structures were displayed on Silicon Graphics using the program InsightII (Dayringer et al., 1986; BIOSYM Corp.,

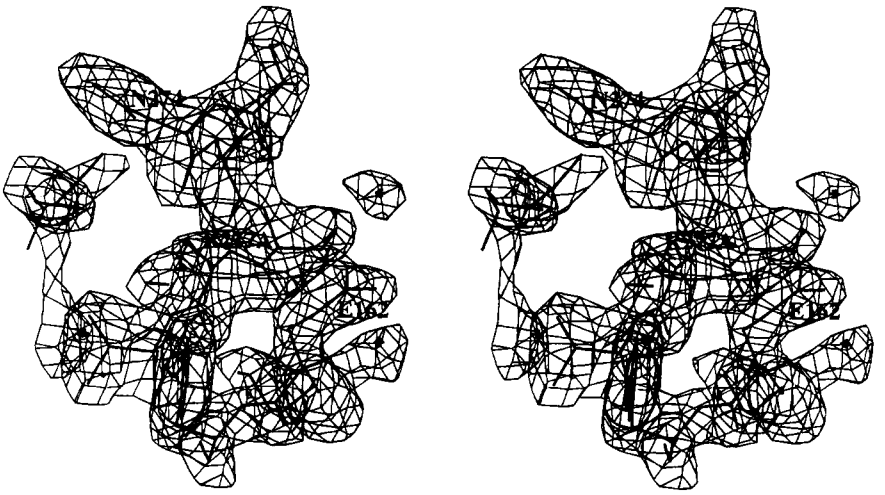

FIGURE 1: Stereoview of a $2F_o - F_c$ map for the R277A mutant. The map is contoured at a level of 1σ above background and centered at residue 277.

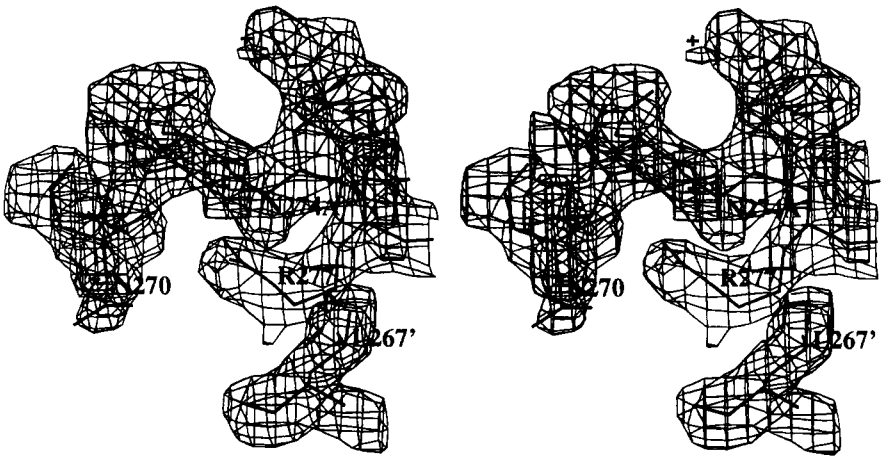

FIGURE 2: Stereoview of a $2F_o - F_c$ map for the N274A mutant. The map is contoured at a level of 1σ above background and centered at residue 274.

Table 2: AMP Activation of Wild-Type Phosphorylase and Mutant Enzymes[a]

enzyme	V_{max} [μmol/(min·mg)]	n_H	$[S]_{0.5[AMP]}$ (μM)
wild-type	29.4 ± 0.3	1.57 ± 0.04	16.5 ± 0.4
N270A	16.3 ± 0.4	1.27 ± 0.06	28 ± 2
N274A	18.1 ± 0.6	1.21 ± 0.06	5.3 ± 0.4
R277A	13.9 ± 0.3	1.27 ± 0.07	38.2 ± 2
YTH	3.49 ± 0.04	1.04 ± 0.03	21.6 ± 0.9

[a] Enzymatic activities were measured at 30 °C at pH 6.8. The concentration of G-1-P was held constant at 10 mM. The kinetic parameters were determined from a nonlinear least-squares fit to the Hill equation.

Table 3: Kinetic Parameters for Wild-Type and Mutant Forms of Phosphorylase[a]

enzyme	V_{max}[b] [μmol/(min·mg)]	n_H	$[S]_{0.5[G\text{-}1\text{-}P]}$ (mM)
wild-type	27.3 ± 0.4	1.67 ± 0.04	0.91 ± 0.02
N270A	10.0 ± 0.9	1.6 ± 0.1	1.5 ± 0.2
N274A	16.1 ± 0.3	1.19 ± 0.04	0.53 ± 0.02
R277A	7.7 ± 0.1	1.48 ± 0.03	0.83 ± 0.02
YTH	2.98 ± 0.03	1.28 ± 0.03	0.49 ± 0.01

[a] Enzymatic activities were measured at 30 °C at pH 6.8. The concentration of AMP was held constant at 50 μM. The kinetic parameters were determined from a nonlinear least-squares fit to the Hill equation. [b] Maximal observed specific activity.

San Diego, CA) and inspected visually. Differences in the configuration of the tower helices and in the orientation of the domains and subunits were further analyzed with the principal axes algorithm using GEM.

RESULTS

Kinetic Analysis of the Mutants. Kinetic characterization of the mutants shows that the substitutions in the tower helix region alter the kinetic and allosteric properties of phosphorylase (Tables 2 and 3). Figure 3 shows Hill plots of AMP saturation curves for the wild-type enzyme and the mutants. The mutant with an alanine at position 274 shows a decrease in AMP cooperativity and a K_a for AMP that is about one-fourth of the value that is observed for the wild-type enzyme. Its apparent V_{max} is about half that of the wild-type enzyme. The mutant with an alanine at position 277 also shows reduced AMP cooperativity, but, in contrast, the K_a for AMP increases about 3-fold over that for the wild-type enzyme. The apparent V_{max} for this mutant is also reduced by about 2-fold. Substitution at 270 diminishes AMP cooperativity as well, but binding of the effector is only slightly weakened. Again, the apparent V_{max} is reduced by about 2-fold. For the mutant with the tower helix region from yeast phosphorylase (YTH), AMP cooperativity is decreased, but the K_a for AMP is similar to that of the wild-type enzyme, and the apparent V_{max} is lowered 8-fold (Table 2).

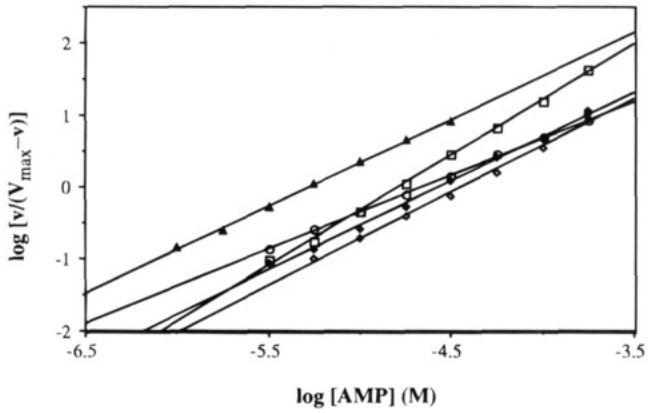

FIGURE 3: Hill plots of kinetic data from AMP saturation curves for (□) wild-type phosphorylase and the (◆) N270A, (▲) N274A, (◇) R277A, and (○) YTH mutants. Assays contained 50 mM BES, pH 6.8, 1 mM EDTA, 1 mM DTT, and 1% glycogen. The concentration of AMP was varied from 0 to 300 μM while the concentration of glucose 1-phosphate was held constant at 10 mM. Activities were measured at 30 °C. Each point represents the average of four measurements.

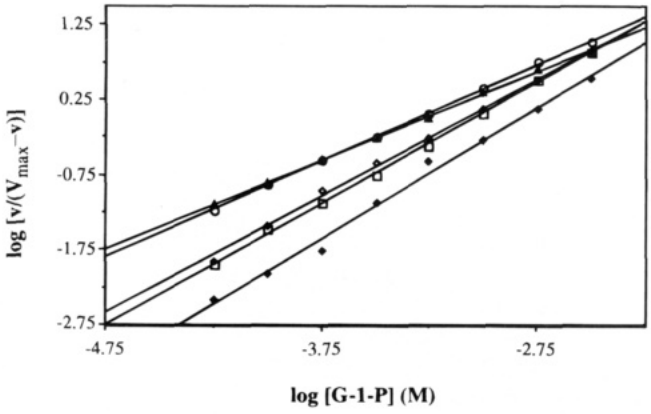

FIGURE 4: Hill plots of kinetic data from glucose-1-phosphate saturation curves for (□) wild-type phosphorylase and the (◆) N270A, (▲) N274A, (◇) R277A, and (○) YTH mutants. Assays contained 50 mM BES, pH 6.8, 1 mM EDTA, 1 mM DTT, and 1% glycogen. The concentration of glucose 1-phosphate was varied from 0 to 10 mM while the concentration of AMP was held constant at 50 μM. Activities were measured at 30 °C. Each point represents the average of four measurements.

Hill plots of glucose 1-phosphate saturation curves for the wild-type and mutant enzymes are shown in Figure 4. The alanine substitution at 274 causes a loss in cooperativity for glucose 1-phosphate and a 2.5-fold reduction in the $[S]_{0.5}$ for glucose 1-phosphate. The N270A and R277A mutants have $[S]_{0.5}$ values and Hill coefficients for glucose 1-phosphate that are comparable to those of the wild-type enzyme. The mutant with the yeast tower helix displays a loss in cooperativity for glucose 1-phosphate, and the $[S]_{0.5}$ for the substrate is reduced 2-fold (Table 3). At the AMP concentration of 50 μM used in these assays, the N274A mutant is saturated with AMP whereas the wild-type enzyme and the other mutants are not. It was therefore of interest to assay the N274A mutant at a subsaturating level of AMP to determine whether homotropic cooperativity for glucose 1-phosphate could be detected. A Hill coefficient of 1.36 for glucose 1-phosphate was obtained from a glucose 1-phosphate saturation curve at 5 μM AMP for this mutant.

Structural Analysis of the Mutants. Structures of the N274A and R277A mutants were compared to two structures

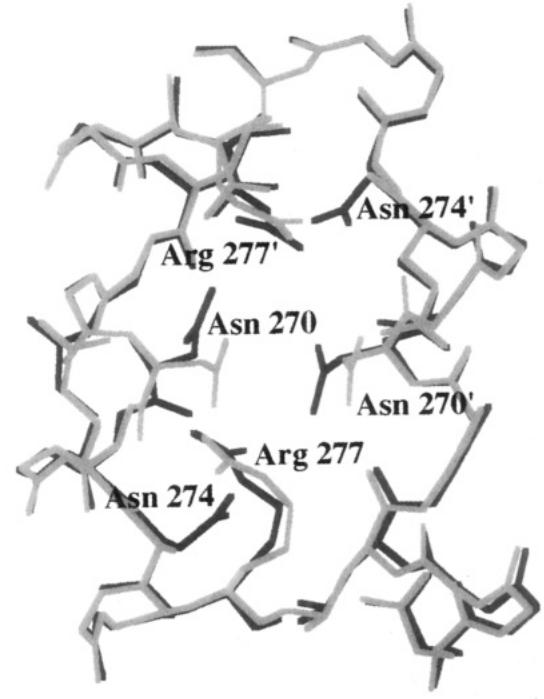

FIGURE 5: Comparison of helix interactions in wild-type phosphorylase (shown in dark gray) and the N274A mutant (shown in light gray). Both tower helices at the dimer interface are shown. The main chain atomic coordinates of residues 264−276 from one helix of the mutant are superimposed on those of the native enzyme (Martin et al., 1990; Brookhaven Protein Data Bank entry 2 GPB).

of glycogen phosphorylase *b* in different conformational states, one inactive (Martin et al., 1990), the other partially activated by AMP (Sprang et al., 1991). The C domains of the monomers for native phosphorylase *b* and the mutants were superimposed, and the rms displacements of the atomic coordinates for backbone atoms were determined for regions of particular interest, namely, the tower helices where mutations were located, the active site gate, and the Cap and α_2 helix, which form the binding site for AMP (Goldsmith et al., 1989). The structures of the mutant enzymes closely resemble the structure of the native enzyme in its inactive conformation, with almost insignificant deviations in atomic positions. For the N274A mutant, a comparison to the inactive native conformer, shows that small shifts, averaging 0.43 Å, in atomic coordinates, occur in the tower helix region (Figure 5). The rms deviation for the Cap and α_2 helix region in this mutant is 0.36 Å, barely above the expected error in the coordinates of 0.2−0.3 Å, and an rms deviation of 0.22 Å for residues of the gate shows that no significant structural change occurs in this region. For the R277A mutant, the largest changes in atomic coordinates are found in the Cap and α_2 helix regions of the activation locus, where residues exhibit an average rms deviation of 0.48 Å (residues 40−78), and in residues 180−190, which have an rms deviation of 0.47 Å. This latter region is unaffected in the N274A mutant which has an rms deviation for these residues of 0.25 Å. The tower helix region in the R277A mutant has an rms deviation of 0.37 Å (Figure 6), barely above the expected error in the coordinates, and the rms deviation of 0.30 Å for residues of the gate shows that the position of this loop of amino acids is not significantly altered.

The relative disposition of domains and the quaternary conformations of the mutants were further evaluated using the principal axes algorithm (Browner et al., 1992). This

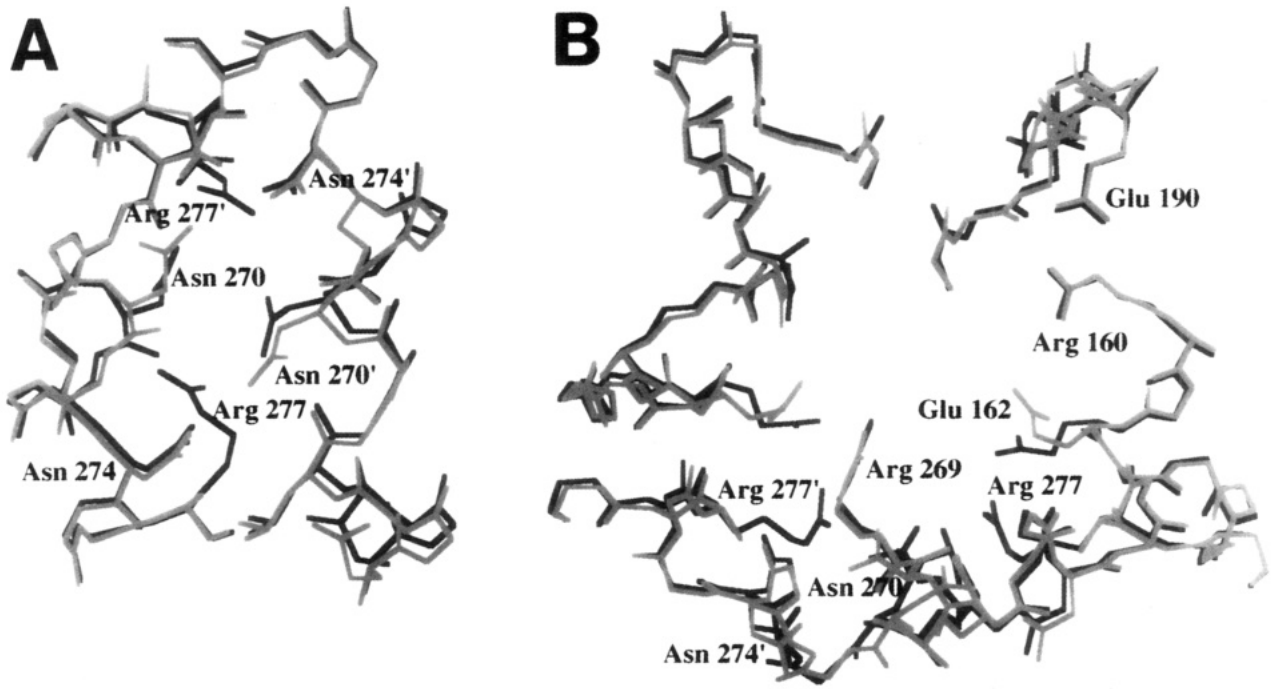

FIGURE 6: Comparison of tower helix interactions in the native enzyme (shown in dark gray) and the R277A mutant (shown in light gray). The main chain atomic coordinates of residues 264−276 from one helix of the mutant are superimposed on those of the native enzyme (Martin et al., 1990; Brookhaven Protein Data Bank entry 2 GPB). Two views of the tower helix region are presented: (A) Differences in the backbone atoms of the helices and the refined positions of sidechains. (B) Changes in contacts with the neighboring β strand (residues 162−165) and, in particular, the movement of Glu 162.

analysis detected no significant changes for either mutant in the separation of the centers of mass of the domains within the dimer when compared to the structure of the inactive native enzyme with the exception that the activation and C-terminal domains separate slightly, perhaps by 0.15 Å, in the R277A structure. This change is probably too small to be considered significant. Differences in the orientations of domains within the dimer were assessed from measurements of the angles formed between principal axes of like domains. For the N274A mutant, the angles between principal axes differed from those of the wild-type enzyme by no more than 0.4° for the activation domains and 0.7° for the N-terminal domains. For the R277A mutant, angular differences were larger for the activation domains, as much as 1.1°, but less than 0.35° for the N-terminal domains. Neither mutant showed significant changes from the native enzyme in the orientations of the C-terminal domains. Angular differences from the native enzyme of less than 0.15° for the principal axes of the C-terminal domains provide an estimate of the level of error in these measurements.

DISCUSSION

Activation of phosphorylase by binding of AMP triggers subunit and domain rotations which reposition the two tower helices located at the dimer interface (Sprang et al., 1987, 1991; Barford & Johnson, 1989; Barford et al., 1991). The large differences in tertiary structure that are observed in the tower helix region in various crystal structures have led to speculation that this region may play a critical role in allosteric regulation. It was suggested that the tower helices through changes in their precise orientation and the specificity of their interactions propagate structural changes from the subunit interface to the active site (Barford & Johnson, 1989). On the other hand, movement of the helices may represent instead a passive response to surrounding quaternary and tertiary structural changes triggered by ligand binding. The alternative packing of the helices may simply be required to accommodate the rotation of the subunits and the domain movements during the allosteric transition. Amino acid replacements were made in the tower helices to test proposals that specific interactions in this region are required for allosteric regulation. If the tower helices play an active role in the allosteric response, mutations in this region might be expected to affect regulatory properties of the enzyme in several ways: Changing packing interactions between the helices could impair coupling between the active sites or weaken the linkage between the AMP site and the active site and interfere with activation. Cooperativity could be sensitive to mutations that affect the stabilities of inactive or active conformers of the enzyme or that alter the relative affinities for ligands in the different conformational states.

Interpreting the kinetic properties of the enzyme variants requires an understanding of the molecular basis for allosteric effects in phosphorylase. Allosteric behavior in proteins has traditionally been explained in terms of either the concerted model of Monod, Wyman, and Changeux (Monod et al., 1965) or the sequential model of Koshland, Nemethy, and Filmer (Koshland et al., 1966). Both models are predicated on the theory that cooperativity derives from ligand-induced changes in protein conformation that alter subunit associations, quaternary structure, and tertiary structure. For many of the kinetic and equilibrium binding studies of phosphorylase to date, the concerted model has been invoked for interpretation of data, in part because of its simplicity. This model restricts the enzyme to two global conformations, an R state with a high affinity for substrates and activators and high catalytic activity and a T state with low affinity for activators and substrates and low catalytic activity. In most cases, kinetic and equilibrium binding data for phosphorylase *b* fit the Monod, Wyman, and Changeux model reasonably

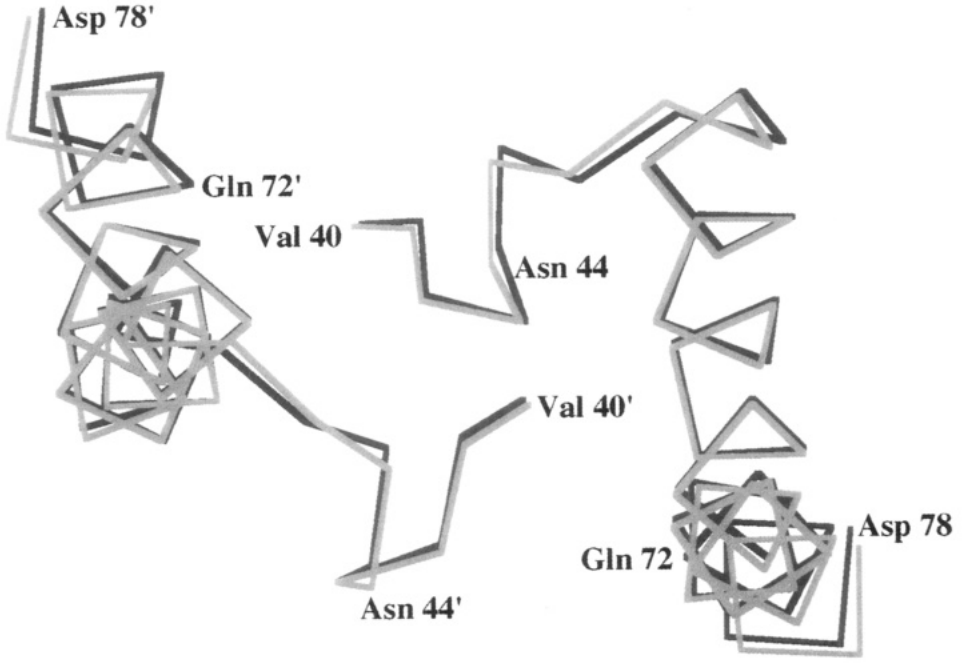

FIGURE 7: Comparison of the activation domains (residues 40−78) of the native enzyme (shown in dark gray) and the R277A mutant (shown in light gray). The main chain atomic coordinates of residues from the C-terminal domain of one subunit of the mutant were superimposed on those of the native enzyme. The program Newdome was used to select residues for the superposition as described in the text. The structures are drawn as α-carbon traces.

well, though some deviations from this model have been discovered [for a review, see Madsen et al. (1976) and Madsen (1986)], and crystallographic studies show that the enzyme can adopt more than two conformational states. In reality, allosteric effects may arise from a conformational continuum of states, each having a particular level of binding affinity and catalytic activity. For the ease of discussion here, however, the kinetic data will be interpreted in terms of a concerted transition between T and R states.

The tower helix region of yeast phosphorylase was substituted for the corresponding region of the muscle enzyme to test the possibility that the tower helices play a relatively minor role in the allosteric response. If large displacements of the helices during the allosteric transition were merely a passive response to surrounding structural changes, the nature of the polypeptide inserted in this region should have little effect on the kinetic properties of the enzyme. The substitution of the tower helix region from the yeast enzyme not only eliminates native interactions but replaces them with an entire set of new interactions. A kinetic analysis of the mutant shows that cooperativity is reduced for both AMP and glucose 1-phosphate, yet the apparent binding affinities of the effector and the substrate are nearly the same as those of the wild-type enzyme (Tables 2 and 3). This mutant still requires AMP for activation, but the maximal specific activity of the enzyme is reduced 8-fold. The dependence on AMP indicates that at least two conformational states, which have differing levels of catalytic activity, are accessible to the protein. The loss in catalytic activity suggests that the mutant cannot achieve the native R state. The replacement of a substantial region of the subunit interface might be expected to perturb the quaternary state of the enzyme. The loss in cooperativity for both glucose 1-phosphate and AMP occurs without a decrease in the apparent binding affinities of either ligand and suggests that the substitution of the yeast tower helix destabilizes the T state for this mutant. Clearly, perturbing the packing interactions between the helices does have long range effects that extend to both the activation site and the active site. The retention of AMP activation, however, with only a modest decrease in specific activity, indicates that replacement of the tower helix region can be tolerated by the enzyme without completely destroying the coupling between the AMP site and the catalytic site. Nevertheless, specific interactions are necessary for achieving the fine balance in conformational states that allows for homotropic cooperativity and native levels of catalytic activity.

In order to test the functions of specific interactions involving residues of the tower helices, alanine substitutions were made at positions 270, 274, and 277. Crystallographic studies show that the pattern of hydrogen-bonding interactions among these residues is altered by changes in the configuration of the helices during the allosteric transition (Figure 8) (Sprang et al., 1987, 1991; Barford & Johnson, 1989; Barford et al., 1991). Amino acid replacements might be expected, therefore, to differentially affect the energetics of subunit associations in different quaternary states of the enzyme. In addition, Barford and Johnson (1989) noted that residues 276−279 form a network of hydrogen bonds with residues of a β-sheet consisting of residues 162−164. Movement of the tower helices perturbs this β-sheet, which in turn displaces residues Asn 133 and Pro 281 at the active site. It was suggested that the tower helices, through specific interactions with this β-sheet, could link structural changes at the subunit interface, induced by AMP binding, to changes at the active site.

The R277A mutant is of particular interest in this regard because its guanidinium group normally forms charged hydrogen bonds with the carboxylate group of Glu 163 of the β-sheet in both inactive and activated states. Surprisingly, this substitution appears to have little functional effect at the active site. The R277A mutant displays cooperativity and an $[S]_{0.5}$ for glucose 1-phosphate that are nearly identical to those of the wild-type enzyme (Table 3). The mutation,

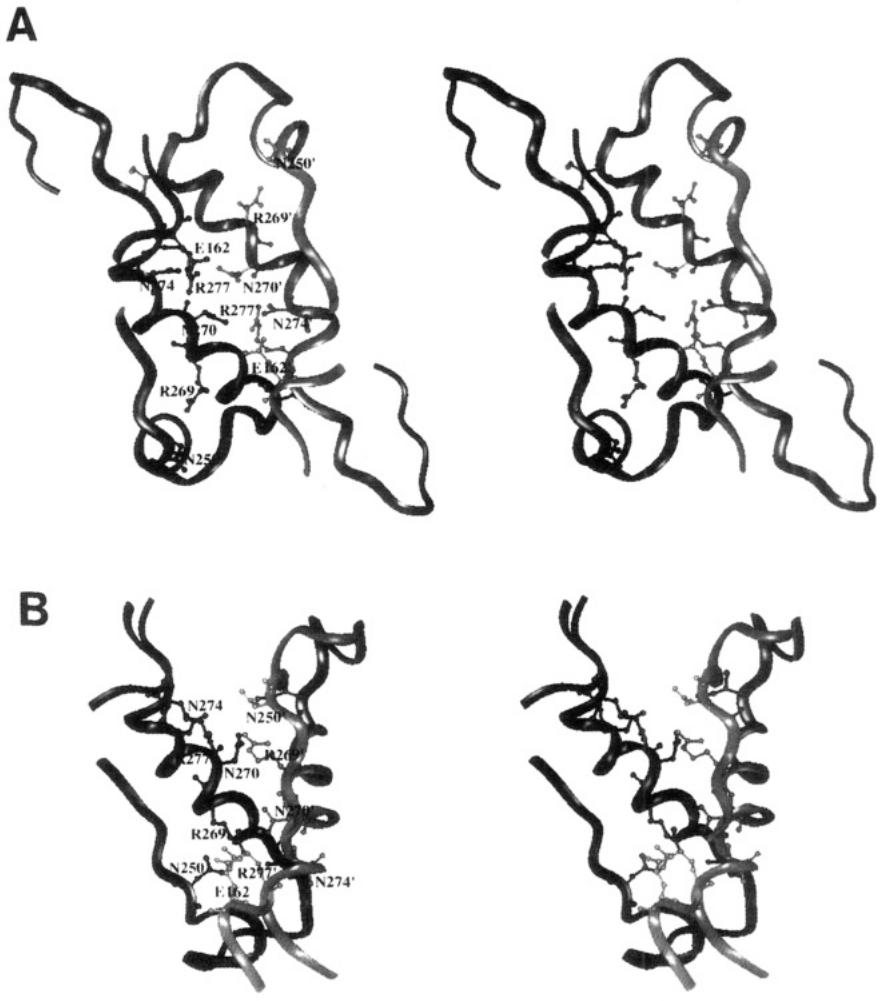

FIGURE 8: Alternative packing interactions at the dimer interface of phosphorylase *b* in inactive and activated conformations. The region of the protein that is shown includes the tower helix (residues 261−275), the preceding β strand (residues 245−249), the parallel β sheet formed from residues 276−279 and 162−165, and the active site gate (residues 280−288). The main chain of the protein is drawn as a ribbon, and selected side chains are shown in a ball-and-stick representation. One subunit is colored dark gray, and the other subunit is colored light gray. (A) Inactive conformation of phosphorylase *b* crystallized in the presence of the inhibitor glucose (Martin et al., 1990; Brookhaven Protein Data Bank entry 2 GPB). (B) Partially activated conformation of phosphorylase *b* crystallized in the presence of ammonium sulfate (Barford & Johnson, 1989; Brookhaven Protein Data Bank entry 9 GPB).

however, does reduce binding affinity and cooperativity for AMP (Table 2). The behavior of the N270A mutant is similar. This mutant shows a reduction in cooperativity for AMP but not for glucose 1-phosphate. AMP binding is weakened while the $[S]_{0.5}$ for glucose 1-phosphate is comparatively unaffected. Although AMP binding is not cooperative in the N270A and R277A mutants, V_{max} is reduced only 2-fold by either substitution and the dependence on AMP for catalytic activity shows that the activation sites and the active sites remain linked. The retention of homotropic cooperativity for glucose 1-phosphate suggests that the energetics of T to R switching are relatively insensitive to these substitutions. The altered regulatory properties of these mutants may be caused by weaker binding of AMP in the R state. Cooperativity for the activator could be lost if the difference in the affinities for AMP in inactive and active conformational states of phosphorylase is diminished.

The structural basis for the elevated K_a and the reduced cooperativity for AMP in the R277A and N270A mutants is not readily apparent from crystallographic studies. The changes in binding of the activator are not the result of a loss of direct interactions between R277 or N270 and residues at the effector site. The AMP site is located about 30 Å away from the tower helix region at the opposite end of the subunit interface. An examination of the electron density map for the R277A mutant in the region surrounding the mutation (Figure 1) reveals small local changes in the positions of individual side chains. The side chain of Asn 270 forms a hydrogen bond with the main chain carbonyl O of Leu 267 and an indirect hydrogen bond through an intervening water molecule with the amide $O_{\delta 1}$ of Asn 274 from the opposite subunit. Loss of the interaction between the guanidinium group of R277 and the carboxylate group of 162 is partially compensated by movement of the carboxylate side chain of Glu 162 closer to the guanidinium group of Arg 160 (Figure 6). In the vicinity of the AMP binding site at the interface between the Cap (residues 42−46) and the α_2 helix (residues 47−78), residues show small changes in position (Figure 7). Residues of the α_2 helix shift on average about 0.48 Å along the helical axis in the direction of the C-terminus. The distance beween the α_2 helix of one subunit and the cap from the opposite subunit, however, is not altered significantly. Although these shifts may reflect a true mispositioning of residues surrounding the AMP binding site, the atomic *B* factors for residues of the cap and α_2 helix indicate that this region is flexible, and the resolution of the R277A crystal structure and the absence of AMP in the crystals preclude any firm conclusions

regarding the structural changes responsible for the loss in binding affinity and cooperativity for AMP.

A comparison of crystallographic structures of the native enzyme in inactive and active conformations indicates that the substitutions at 270 and 277 should destabilize both T and R quaternary states (Figure 8). Structures of phosphorylase *b* in the inhibited state show that the side chain of Arg 277 makes a direct intersubunit hydrogen bond with the side chain of N270. In the structure of the activated enzyme, the guanidinium group of Arg 277 forms an intersubunit hydrogen bond with the side chain of Asn 250 whereas Asn 270 forms an intersubunit hydrogen bond with Arg 269. Altered packing interactions on the catalytic side of the dimer interface may, therefore, indirectly perturb interactions at the effector site in both the T and R states of the R277A and the N270A mutants.

The alanine substitution at residue 274, in contrast to the other mutations, appears to selectively destabilize the inactive quaternary state. Kinetic analysis of the N274A mutant shows that it has a higher affinity for AMP and glucose 1-phosphate and decreased cooperativity for both the activator and the substrate (Tables 2 and 3). The mutation does not completely abolish homotropic coupling between the active sites; however, cooperativity for glucose 1-phosphate can be detected only at lower concentrations of AMP than for the wild-type enzyme. The decrease in the K_a for AMP indicates that less binding energy is required to promote the R state. Crystallographic studies show that when the native enzyme is in an inactive conformation, the amide $O_{\delta 1}$ of Asn 274 forms an intrasubunit hydrogen bond with the guanidinium group of 277, which in turn interacts with the side chain of Asn 270 of the opposite subunit (Martin et al., 1990). Loss of these interactions is expected to reduce the subunit interaction energy in the inactive state. In crystal structures in which the native enzyme is partially activated, this interaction between Asn 274 and R277 is absent and Asn 274 does not make any intersubunit contacts (Figure 8) (Barford & Johnson, 1989; Barford et al., 1991; Sprang et al., 1991). Inspection of the crystal structure of the N274A mutant indicates that the side chains of Asn 270 and Arg 277 are engaged exclusively in intrasubunit hydrogen bonds (Figure 5). Asn 270 forms hydrogen bonds with the main chain N of Leu 271 and the carbonyl O of Leu 267. The guanidinium group of Arg 277 forms hydrogen bonds with the main chain carbonyl O of Glu 273 and the carboxylate group of Glu 162. By selectively destabilizing subunit interactions in the inactive conformer, the N274A mutation may lower the energy barrier for quaternary switching from T to R states.

The combined mutagenesis studies show that the tower helices participate in specific interactions which influence homotropic and heterotropic cooperativity and the regulation of enzymatic activity. The energetics of allosteric switching between conformational states are affected by substitutions in the helices, which weaken and alter subunit interactions and differentially perturb the stabilities of inactive and active conformational states. The affinity of AMP binding at the opposite end of the dimer interface is also sensitive to changes in contacts between the helices. Curiously, the liver and brain isozymes of phosphorylase exhibit regulatory properties which are distinct from the muscle enzyme, yet the three isozymes share a conserved tower helix region (Hudson et al., 1993). Unique regulatory properties have apparently evolved from substitutions in diverse regions of the molecule, the tower helix region representing only a component of the allosteric switch. The mutagenesis studies here support speculation that movement of the tower helices during the allosteric transition plays a role in coupling the effector sites and active sites and that specific interactions with residues of the helices may indeed determine the precise allosteric response.

ACKNOWLEDGMENT

We thank Dr. P. Hwang for his critical reading of the manuscript.

REFERENCES

Barford, D., & Johnson, L. N. (1989) *Nature 340,* 609−616.
Barford, D., Hu, S. H., & Johnson, L. N. (1991) *J. Mol. Biol. 218,* 233−260.
Browner, M. F., & Fletterick, R. J. (1992) *Trends Biochem. Sci. 17,* 66−71.
Browner, M. F., Rasor, P., Tugendreich, S., & Fletterick, R. J. (1991) *Protein Eng. 4,* 351−357.
Browner, M. F., Fauman, E. B., & Fletterick, R. J. (1992) *Biochemistry 31,* 11297−11304.
Brunger, A. T. (1987) *Science 235,* 458−460.
Buc, M. H., Ullmann, A., Goldberg, M., & Buc, H. (1971) *Biochimie 53,* 283−289.
Carney, I. T., Beynon, R. J., Kay, J., & Birket, N. (1978) *Anal. Biochem. 85,* 321−324.
Cohen, P. (1989) *Annu. Rev. Biochem. 58,* 453−508.
Cori, C. F., & Cori, G. T. (1936) *Proc. Soc. Exp. Biol. Med. 34,* 702−705.
Cori, G. T., & Cori, C. F. (1940) *J. Biol. Chem. 135,* 733−756.
Cori, G. T., & Green, A. A. (1943) *J. Biol. Chem. 151,* 31−38.
Dayringer, H., Tramontano, A., Sprang, S., & Fletterick, R. J. (1986) *J. Mol. Graphics 4,* 82−91.
Eagles, P. A., Iqbal, M., Johnson, L. N., Mosley, J., & Wilson, K. S. (1972) *J. Mol. Biol. 71,* 803−806.
Fischer, E. H., & Krebs, E. J. (1955) *J. Biol. Chem. 216,* 121−132.
Fischer, E. H., Graves, D. H., & Krebs, E. G. (1957) *Fed. Proc. 16,* 180.
Fischer, E. J. H., Graves, D. J., Crittenden, E. R. S., & Krebs, E. H. (1959) *J. Biol. Chem. 234,* 1698−1704.
Fletterick, R. J., & Madsen, N. B. (1980) *Annu. Rev. Biochem. 49,* 31−61.
Fletterick, R. J., & Sprang, S. R. (1982) *Acc. Chem. Res. 15,* 361−369.
Fletterick, R. J., Burke, J. A., Hwang, P. K., Nakano, K., & Newgard, C. B. (1986) *Ann. N.Y. Acad. Sci. 478,* 220−232.
Fosset, M., Muir, L. W., Nielsen, L. D., & Fischer, E. H. (1971) *Biochemistry 10,* 4105−4113.
Goldsmith, E. J., Sprang, S. R., Hamlin, R., Xuong, N. H., & Fletterick, R. J. (1989) *Science 245,* 528−532.
Huang, C. Y., & Graves, D. J. (1970) *Biochemistry 9,* 660−671.
Hudson, J. W., Hefferon, K. L., & Crerar, M. M. (1993) *Biochim. Biophys. Acta 1164,* 197−208.
Hwang, P. K., & Fletterick, R. J. (1986) *Nature 324,* 80−84.
Ingebritsen, T. S., & Cohen, P. (1983) *Science 221,* 331−338.
Johnson, L. N. (1992) *FASEB J. 6,* 2274−2282.
Johnson, L. N., & Barford, D. (1990) *J. Biol. Chem. 265,* 2409−2412.
Johnson, L. N., Hajdu, J., Acharya, K. R., Stuart, D. I., McLaughlin, P. J., Oikonomakos, N. G., & Barford, D. (1989) in *Allosteric Enzymes*, CRC Press Inc., Boca Raton, FL.
Kabsch, W. (1988) *J. Appl. Crystallogr. 21,* 916−924.
Kihlman, B., & Overgaard-Hansen, K. (1955) *Exp. Cell. Res. 8,* 252−255.
Koshland, D., Jr., Nemethy, G., & Filmer, D. (1966) *Biochemistry 5,* 365−385.
Krebs, E. G. (1972) *Curr. Top. Cell. Regul. 5,* 99−133.
Krebs, E. G., & Fischer, E. H. (1956) *Biochim. Biophys. Acta 20,* 150−157.

Luong, C. B., Browner, M. F., Fletterick, R. J., & Haymore, B. L. (1992) *J. Chromatogr. 584,* 77−84.
Madsen, N. B. (1986) *The Enzymes XVII,* 365−394.
Madsen, N. B., Avramovic-Zikic, O., Lue, P. F., & Honikel, K. O. (1976) *Mol. Cell. Biochem. 11,* 35−50.
Martin, J. L., Johnson, L. N., & Withers, S. G. (1990) *Biochemistry 29,* 10745−10757.
Monod, J., Wyman, J., & Changeux, J.-P. (1965) *J. Mol. Biol. 12,* 88−118.
Morgan, H. E., & Parmeggiani, A. (1964) *J. Biol. Chem. 239,* 2440−2445.
Parmeggiani, A., & Morgan, H. E. (1962) *Biochem. Biophys. Res. Commun. 9,* 252−256.
Perry, K. M., Fauman, E. B., Finer-Moore, J. S., Montfort, W. R., Maley, G. F., Maley, F., & Stroud, R. M. (1990) *Proteins 8,* 315−333.
Sack, J. S. (1988) *J. Mol. Graphics 6,* 224−225.
Sprang, S., Goldsmith, E., & Fletterick, R. (1987) *Science 237,* 1012−1019.
Sprang, S. R., Acharya, K. R., Goldsmith, E. J., Stuart, D. I., Varvill, K., Fletterick, R. J., Madsen, N. B., & Johnson, L. N. (1988) *Nature 336,* 215−221.
Sprang, S. R., Withers, S. G., Goldsmith, E. J., Fletterick, R. J., & Madsen, N. B. (1991) *Science 254,* 1367−1371.
Sprang, S. R., Madsen, N. B., & Withers, S. G. (1992) *Protein Sci. 1,* 1100−1111.
Titani, K., Koide, A., Hermann, J., Ericsson, L. H., Kumar, S., Wade, R. D., Walsh, K. A., Neurath, H., & Fischer, E. H. (1977) *Proc. Natl. Acad. Sci. U.S.A. 74,* 4762−4766.
Withers, S. G., Madsen, N. B., Sprang, S. R., & Fletterick, R. J. (1982) *Biochemistry 21,* 5372−5382.

BI9424813